

Absolute measurement of vacuum ultraviolet photon flux in an inductively coupled plasma using a Au thin film

Cite as: J. Vac. Sci. Technol. B 40, 022206 (2022); <https://doi.org/10.1116/6.0001709>

Submitted: 22 December 2021 • Accepted: 31 January 2022 • Published Online: 25 February 2022

Linfeng Du, Paul Ruchhoeft,  Demetre J. Economou, et al.



View Online



Export Citation



CrossMark





Instruments for Advanced Science

- Knowledge,
- Experience,
- Expertise

Click to view our product catalogue

Contact Hiden Analytical for further details:

 www.HidenAnalytical.com
 info@hideninc.com

Gas Analysis



- ▶ dynamic measurement of reaction gas streams
- ▶ catalysis and thermal analysis
- ▶ molecular beam studies
- ▶ dissolved species probes
- ▶ fermentation, environmental and ecological studies

Surface Science



- ▶ UHVTPD
- ▶ SIMS
- ▶ end point detection in ion beam etch
- ▶ elemental imaging - surface mapping

Plasma Diagnostics



- ▶ plasma source characterization
- ▶ etch and deposition process reaction kinetic studies
- ▶ analysis of neutral and radical species

Vacuum Analysis



- ▶ partial pressure measurement and control of process gases
- ▶ reactive sputter process control
- ▶ vacuum diagnostics
- ▶ vacuum coating process monitoring



Absolute measurement of vacuum ultraviolet photon flux in an inductively coupled plasma using a Au thin film

Cite as: J. Vac. Sci. Technol. B 40, 022206 (2022); doi: 10.1116/6.0001709

Submitted: 22 December 2021 · Accepted: 31 January 2022 ·

Published Online: 25 February 2022



Linfeng Du,¹ Paul Ruchhoeft,^{2,a)} Demetre J. Economou,^{1,b)}  and Vincent M. Donnelly^{1,c)} 

AFFILIATIONS

¹Plasma Processing Laboratory, William A. Brookshire Department of Chemical and Biomolecular Engineering, University of Houston, Houston, Texas 77204

²Department of Electrical and Computer Engineering, University of Houston, Houston, Texas 77204

Note: This paper is a part of the Special Topic Collection on Plasma Processing for Advanced Microelectronics.

^{a)}Electronic mail: pruchhoeft@uh.edu

^{b)}Electronic mail: economou@uh.edu

^{c)}Electronic mail: vmdonnelly@uh.edu

ABSTRACT

A new method for absolute measurement of the vacuum ultraviolet (VUV) photon flux at the edge of a plasma is described. The light produced by the plasma was allowed to strike a negatively biased, gold-coated copper substrate remote from the plasma. The resulting photoelectron emission current was measured, and the absolute photon flux was then found from the known photoelectron yield of Au. The method was used to quantify the amount of VUV light produced by an Ar/He inductively coupled plasma (ICP). Strong emissions at 104.82 and 106.67 nm, corresponding to the $1s_2$ and $1s_4$ resonant states of Ar, were observed. The maximum, integrated VUV photon flux measured at the remote location was 3.2×10^{13} photons/cm² s. This was estimated to correspond to a flux of 5×10^{15} photons/cm² s at the edge of the ICP, in the range of reported values under similar conditions.

Published under an exclusive license by the AVS. <https://doi.org/10.1116/6.0001709>

I. INTRODUCTION

Low temperature plasmas are widely used in microelectronics fabrication.¹ In addition to electrons, ions, and radicals, the plasma also produces electromagnetic radiation in the infrared to vacuum ultraviolet (VUV) regions. Energetic enough photons can break chemical bonds in the gas phase and on a surface, as well as create electron-hole pairs in the near-surface region of semiconductors, including Si.^{2,3} Surface irradiation can lead to various reactions such as photodesorption of products⁴⁻⁶ and damage to substrates,⁷⁻¹⁰ as well as to thin films, including photoresist and other organic materials.¹¹⁻¹³ Plasma-generated photons can also be used to enhance processes. For example, etching stimulated by VUV photons in a chlorine plasma was used to achieve extremely selective etching of silicon over a thin native oxide layer.¹⁴ Photons can enhance the Si oxidation rate in an oxygen plasma by faster oxygen negative ion migration under irradiation by UV light.^{15,16}

VUV photons are also useful for medical sterilization.¹⁷ In many cases, however, they are detrimental. This is the case for photo-assisted etching (PAE) of Si, where crystallographic etching results in sloped (111) sidewalls on (100) surfaces masked along (110) directions.^{18,19} The self-limiting atomic layer etching process is also hindered by fast etching in the presence of VUV light, even when no bias is applied to the substrate.^{18,20-23} To better understand the mechanism of reactions stimulated by these energetic photons, their etching yield (etched Si atoms-per-photon) should be determined, requiring a measurement of absolute incident photon flux.

The fundamentals of generation and propagation of VUV light in Ar-containing plasmas (argon is a common carrier gas in plasma processing) have been widely studied by experiments and numerical simulations.^{10,24-29} The most intense VUV Ar emissions correspond to the resonant transitions from the $1s_2$ and $1s_4$ states (Paschen notation) to the ground state, with respective energies of

11.83 eV at 104.82 nm and 11.62 eV at 106.67 nm. Absolute photon flux measurements were usually done by placing a VUV photodiode in an adjacent, differentially pumped chamber separated from the main plasma generation chamber by either a small pinhole or a short wavelength cut-off window (e.g., MgF₂). The installation and calibration of photodiodes reduces the feasibility and increases the complexity of this measurement, while any window limits the range of wavelengths detected (e.g., MgF₂ does not transmit Ar 106 nm emission).

In this work, a new method is presented for absolute measurements of the intensity of plasma-produced VUV light by recording the electron photoemission current produced when light from the plasma was incident on a Au thin film deposited on a Cu substrate. The main motivation for this study was to make *in situ* measurements for conditions used in other studies of VUV photo-assisted etching of Si in a Cl₂/Ar plasma, allowing absolute quantum yields (Si atoms-per-photon) to be determined, as reported in Paper II.¹⁹ VUV emission spectra were also recorded under the same conditions.

II. EXPERIMENT

The experimental systems used in this study are shown schematically in Figs. 1(a) and 1(b). The VUV source was a compact ICP generated in a water-cooled alumina tube (19.5 cm long, 3.56 cm inside diameter) and was powered by a 3-turn water-cooled copper coil. The VUV source was either connected directly to a differentially pumped VUV monochromator [Fig. 1(a)] or to a chamber used for in-plasma photo-assisted etching of Si^{-22,23} [Fig. 1(b)]. In the experiments presented here, the ICP source in the etching chamber was always off. In the configuration in Fig. 1(a), no gas was injected downstream of the VUV source, while for the tandem system shown in Fig. 1(b), Ar flow was added to the downstream chamber.

The VUV source was sustained by 13.56 MHz power, either cw, or with 5 kHz pulsed power with a 50% duty cycle, produced by a function generator (BNC, Model 645) and an RF amplifier (ENI, A500). Power in the range between 50 and 200 W was supplied through a T-matching network. The forward and reflected powers were measured with in-line power meters (Bird model 43). Plasma was confined to the VUV source chamber by a grounded tungsten mesh (230 μm square openings, 81% transparency), followed by a bundle of 31 quartz tubes (each 5 mm OD, 4 mm ID, and 30 mm-long) arranged in a honeycomb configuration with a bundle diameter of ~40 mm and ~50% open area.

Ar (Matheson, 99.999% purity) and He (Advanced Specialty Gases, 99.999% purity) flows were regulated by mass flow controllers (MKS Model 1179A) and fed to the VUV source plasma. Ar was also sometimes injected into the downstream chamber. The pressure was measured with a capacitance manometer (MKS 629, 0.1 Torr full scale) in the position indicated in Fig. 1(b). Using ionization gauges, base pressures of ~2.0 × 10⁻⁶ and ~2.0 × 10⁻⁷ Torr were measured in the systems shown in Figs. 1(a) and 1(b), respectively. The gas fed into the VUV source chamber flowed through the honeycomb separator into the downstream chamber and, thus, did not have its own vacuum pump.

Pressure in the downstream region was either 15 or 60 mTorr, and was changed by throttling the gate valve just above the turbomolecular pump, and/or by adjusting the gas flow rates into the

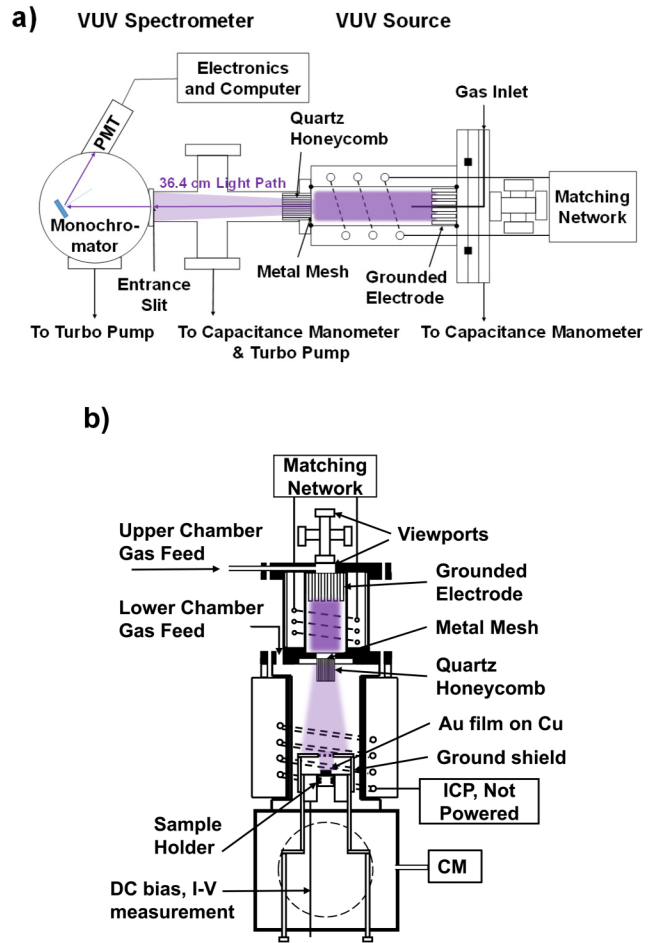


FIG. 1. Schematics of (a) VUV source connected to a differentially pumped VUV monochromator and (b) VUV source in tandem with the etching chamber. Plasma was confined in the VUV source by a metal mesh and a bundle of capillary tubes in a honeycomb configuration. TMP, turbomolecular pump; PMT, photomultiplier tube; CM, capacitance manometer.

VUV source and downstream chamber. Poiseuille's law for laminar flow (with a modification for the dependence of volumetric flow rate on pressure, assuming the ideal gas law) was used to estimate the pressure in the VUV source,³⁰

$$Q_o/N = \frac{\pi D^4}{256\mu L} \frac{P_u^2 - P_d^2}{P_u}, \quad (1)$$

where Q_o is the volumetric flow rate into the VUV source (upper reactor) at a pressure P_u , $L = 3$ cm is the length of the glass tube bundle, $N = 31$ is the number of tubes in the bundle, $D = 0.4$ cm is the tube internal diameter, μ is the gas viscosity, and P_d is the pressure at the tube outlet (the pressure in the etching chamber).

measured by the capacitance manometer downstream from the etching chamber, corrected for an additional small pressure drop). The viscosity of He at 500 K ($\mu = 2.73 \times 10^{-4}$ P) was used, since the feed gas was mostly He and the viscosity of He is nearly the same as that of Ar. For a flow rate of 47.5 SCCM He and 2.5 SCCM Ar into the upper chamber, and an added downstream flow of 250 SCCM Ar, a pressure of $P_d = 60$ mTorr was established. With this condition, the VUV source pressure computed from Eq. (1) was $P_u = 277$ mTorr.

A VUV spectrometer (McPherson model 234/302) was installed downstream of the plasma VUV source [Fig. 1(a)], covering the spectral range from 50 to 280 nm. The spectrometer has a 2400 grooves/mm platinum-coated grating that has an efficiency of 4% at 50 nm, rising to a near-constant 7.5% between 60 and 120 nm, and then falling to a near-constant 3% at 200 nm. The distance from the downstream end of the quartz honeycomb to the entrance slit of the monochromator (36.4 cm light path) matched that from the honeycomb to the Au film in the configuration shown in Fig. 1(b). Survey spectra were collected by scanning over the wavelength range of 50–280 nm, with a spectral resolution of 0.3 nm (150 μ m slit widths). High resolution spectra (used to integrate the intensities of the Ar VUV emission lines) were obtained in the range of 80–130 nm with a resolution of 0.1 nm (50 μ m slit widths). The voltage on the photomultiplier tube (Hamamatsu model R6095, coated with a sodium salicylate scintillator) was -675 V. The relative quantum efficiency of the this VUV detector, determined by the scintillator, is constant between 30 and 120 nm, and then rises slightly ($\sim 20\%$) between 120 and 160 nm.³¹ Between 121 and 254 nm, it has been reported to be constant or increase by $\sim 70\%$.³¹

Absolute photon fluxes at the substrate position [Fig. 1(b)] were determined from photoelectron currents resulting from illumination of a Au-coated Cu sample with light from the plasma. These measurements were used to compute Si etching yields for VUV photons in a chlorine-containing plasma, as reported elsewhere.¹⁹ The photoelectron detection sample consisted of a 100 nm Au film on top of 15 nm-thick NiCr adhesion layer that was deposited on a ~ 2 cm diameter Cu disk using an in-house thermal evaporator. The system consisted of a rectangular chamber pumped by a 2-in. diffusion pump to a base pressure of about 4×10^{-6} Torr. The sample was mounted on a chuck that was placed about 12 in. from the metal source. NiCr and Au pellets were placed into two alumina-coated tungsten baskets (R.D. Mathis Co.) and sequentially heated by a high-current AC source to deposit the two films. A quartz crystal monitor (Kurt J. Lesker FTM-2400) was used to measure the deposition rates of the films, which were maintained at about 0.5 nm/s. A manual shutter was used to control the film thickness.

The coated Cu disk was bonded to the stainless steel sample holder with silver paste. The resistance between the gold surface and the sample holder was $\sim 0.5 \Omega$. Current was measured as a function of DC voltage on the substrate, using a bank of 1.5 and 9 V batteries. A grounded stainless steel “cage” (5 cm outer diameter, 0.3 cm height, with a 2.54 cm diameter opening at the top) surrounded the Au sensor, as shown in Fig. 1(b), providing a return path for the generated photoelectrons and preventing charging of exposed insulating parts. The opening at the top of the cage was

covered with a tungsten mesh (230 μ m square openings, 81% transparency). For cw plasma experiments, the nA-level currents through the Au film were measured by a picoammeter (Keithley 6485). For the pulsed-power experiments, currents were recorded using an oscilloscope (Agilent, DSO 7034B) to measure the voltage-drop across a 1.04 k Ω precision resistor.

The absolute VUV flux was then found from the known photo-electric yield of Au as a function of wavelength. As discussed in more detail below, the photoelectric yield of gold is ~ 0.07 at ~ 105 nm,³² near the most intense Ar VUV lines, but it is more than two orders of magnitude lower at 200 nm and still lower at longer wavelengths.³³ The photoelectron current was measured for both continuous wave (cw) and pulsed plasma operation of the VUV source.

III. RESULTS AND DISCUSSION

A. Argon VUV emission intensity

Emission spectra of the VUV source are shown in Figs. 2(a) and 2(b). Figure 2(a) shows a low resolution spectrum from 50 to 280 nm of a typical plasma contained strong emissions from Ar, weaker N, and H Lyman- α [Fig. 2(a)] from impurities, and very weak He emission at 58.43 nm, corresponding to decay from the 2p state to the ground state. The weak He emission is due to the much higher excitation energies required to populate emitting levels of He. The most intense emissions are from the Ar 1s₄ resonant state at 106.67 nm ($3s^2 3p^5(^2P_{3/2}^o)4s^2[3/2]_1^o \rightarrow 3s^2 3p^6(^1S_0)$) with a photon energy of 11.62 eV, and the 1s₂ resonant state at 104.82 nm ($3s^2 3p^5(^2P_{1/2}^o)4s^2[1/2]_1^o \rightarrow 3s^2 3p^6(^1S_0)$) with a photon energy of 11.83 eV. Higher resolution (0.1 nm) spectra such as that from 80 to 130 nm in Fig. 2(b) also reveal five weak Ar peaks corresponding to radiative decay from higher energy states: 2s₂ at 86.9 nm, 2s₄ at 87.9 nm, 3d₁ at 86.7 nm, 3d₂ at 87.6 nm, and 3d₅ at 89.4 nm. Moreover, two relatively strong Ar⁺ emissions can be seen at 92.0 and 93.2 nm.

Figure 3 shows the intensities of the most important Ar VUV emissions at 104.82 and 106.67 nm, obtained by the integration of the peaks in high resolution spectra like that in Fig. 2(b), as a function of Ar percentage in the Ar/He feed gas at plasma powers in the VUV source of 100, 150, and 200 W. For $\leq 20\%$ Ar, the intensity of the 106.67 nm line was \sim five times stronger than the 104.82 nm peak, and increased with plasma power. The 106.67 nm intensity maximized near 5% Ar or at an Ar partial pressure of about 15 mTorr. Near 50% Ar, the intensity of both lines was nearly equal and had a relatively small dependence on power. At 100% Ar (and lower pressure), the intensity of both lines decreased slightly, with the 104.82 nm line weakly decreasing with increasing power.

B. In situ photocurrent measurement

To find the absolute photon flux from the VUV source in tandem with the etching chamber, the photoelectron current produced by light striking the Au film was measured [Fig. 1(b)]. Absolute photoelectron yields for Au, Y_{pe}^{Au} , defined as the number of electrons ejected from the surface divided by the number of incident photons, have been reported by several researchers. Cairns

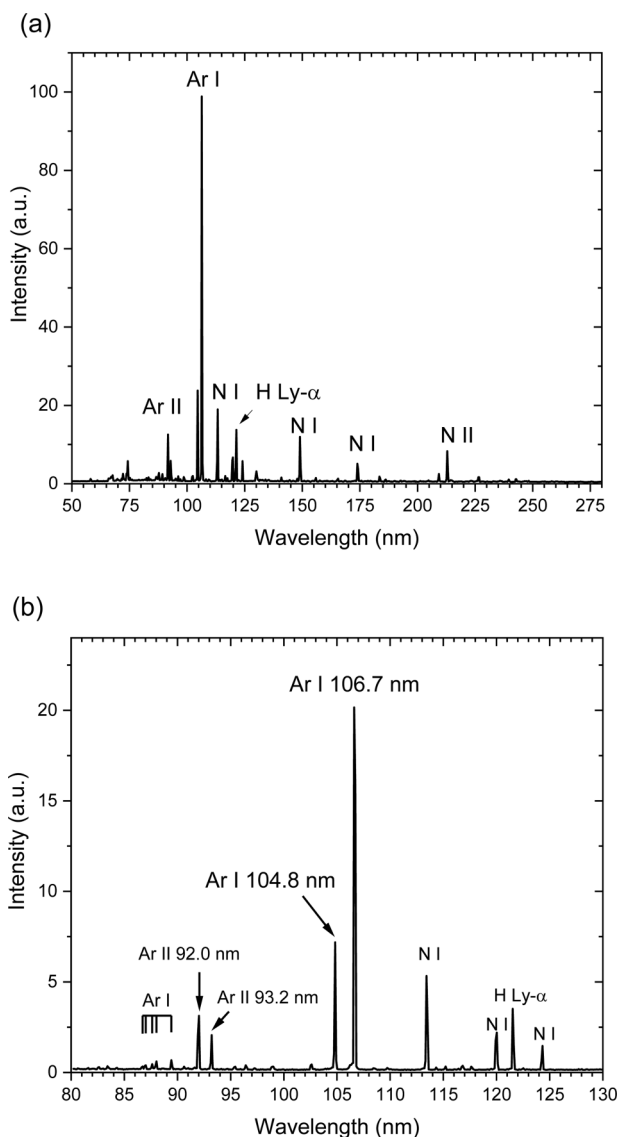


FIG. 2. Optical emission spectra of a 5 SCCM Ar/45 SCCM He plasma at 150 W in the VUV source. The measured downstream pressure was 100 mTorr and the estimated pressure in the VUV source was ~ 310 mTorr. (a) 50–280 nm survey spectrum, and (b) 80–130 nm high resolution spectrum.

and Samson measured yields for gold in the wavelength range of 20–221 nm (62–10.4 eV).³² A maximum yield of 0.13 was found at 80 nm (15.5 eV). At 105.7 nm (11.7 eV), the average wavelength of the strongest 104.82 and 106.67 nm Ar emission lines, $Y_{pe}^{Au} = 0.063$. At the other wavelengths with significant emissions (~ 92.5 nm, the average of the two strongest Ar II lines and 113.5 nm, for N impurity), $Y_{pe}^{Au} = 0.10$ and 0.039, respectively. These values are in excellent agreement with the yields measured by Feuerbacher and Fitton³⁴ (maximum of 0.13 at 17 eV and 0.06

at 11.7 eV). Krolikowski and Spicer reported measured and computed yields (defined as the number of photoelectrons divided by the number of *absorbed* photons) between 107.8 nm (11.5 eV) and 225 nm (5.5 eV).³³ Their measured and computed values were in excellent agreement throughout the energy range investigated, deviating by a maximum of $\sim 20\%$ at 11.5 eV. Extrapolating slightly their measured value at 11.5 eV and converting to incident and not absorbed photons (using a Au reflectivity of $\sim 15\%$ at 11.7 eV³⁵) provides a yield of 0.02 at 11.7 eV, i.e., much lower than the other measurements cited. Both Feuerbacher and Fitton³⁴ and Krolikowski and Spicer³³ found that the photoemission yield falls off rapidly with increasing wavelength to $\sim 10^{-4}$ near 200 nm. Since no photoelectrons are emitted as a result of the strong emission from Ar in the red-near-infrared region, and the other VUV Ar emissions are weak, we attributed all the Au photoemission signal to the 104.82 and 106.67 nm emission lines and used a value of 0.048 for the yield (the average of the three reported measurements).

Before installing the stainless steel cage, photoemission currents measured as a function of substrate bias showed no clear saturation. This was attributed to the ill-defined return path for ejected electrons since the substrate is surrounded by an alumina tube that can charge up. Nonetheless, this bare-substrate configuration allowed sputter-cleaning of the Au surface by operating the lower ICP [Fig. 1(b)] in Ar and negatively biasing the substrate (-50 V for 10 s). Photocurrents measured after sputter-cleaning with just the remote plasma and -25 to -45 V bias were indistinguishable from measurements before cleaning. Thus, it was concluded that any surface contamination had little impact on the photoemission measurements with the grounded cage in place.

Figure 4 shows the current through the gold thin film for a pulsed-power VUV source ICP. As power was turned on, the measured photoelectron current rapidly increased from 10% to 90% of its steady-state value in $13 \mu\text{s}$. This is the characteristic time of electron temperature rise in a pulsed plasma as power is turned on.³⁶ In the plasma off period (afterglow), the current dropped from 90% to 10% in $\sim 20 \mu\text{s}$ to a small steady current of an unknown origin (perhaps a small leakage current). The decay time for emission was attributed to the loss rate of Ar $1s_3$ and $1s_5$ metastables due to collisions with electrons that mostly result in population of the $1s_2$ and $1s_4$ emitting levels. The rate constants for these processes range from 4×10^{-8} ($1s_5 \rightarrow 1s_2$) to $1 \times 10^{-7} \text{ cm}^3 \text{ s}^{-1}$ ($1s_3 \rightarrow 1s_2$) between $T_e = 0.5$ and 1 eV.³⁷ Hence for an electron density near 10^{12} cm^{-3} , emission would be expected to decay with a lifetime of ~ 10 – $20 \mu\text{s}$.

The time response in Fig. 4 is 1000 times faster than the ~ 13 ms for free diffusion of any positive ions that pass through the separator between the VUV source and the etching chamber and reach the substrate. Therefore, stray positive ions did not contribute to the photoelectron current. Likewise, stray electrons cannot reduce the measured current since the substrate was negatively biased at a voltage well beyond the energy expected for electrons diffusing from the remote source. Consequently, we concluded that the current measured in pulsed or steady-state remote plasma operation is a result of photoemission by VUV photons.

All other photoemission measurements reported here were carried out with a continuous wave powered VUV source and the grounded cage in place. Figure 5 shows current as a function of bias

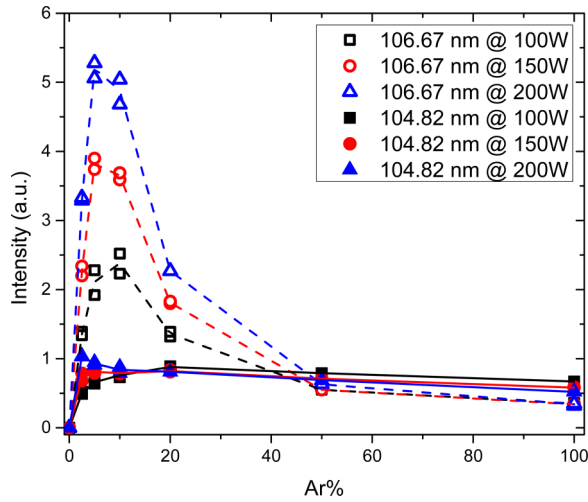


FIG. 3. Ar VUV emission intensity at 104.82 and 106.67 nm as a function of Ar percentage in Ar/He feed gas, at different plasma powers in the VUV source [Fig. 1(a)]. The total gas flow rate was 50 SCCM except for 100% Ar for which the flow rate was 25 SCCM. The measured downstream pressure was kept at 100 mTorr by throttling a gate valve (pressure in the VUV source was estimated to be 310 mTorr, except for 100% Ar, where it was 237 mTorr).

voltage for one set of conditions. A saturated photoelectron current of 260 nA was measured in the voltage range of -9 to -20 V. At more positive voltages stray electrons begin to reduce the current, while more negative voltages likely produced Ar^+ through collisions

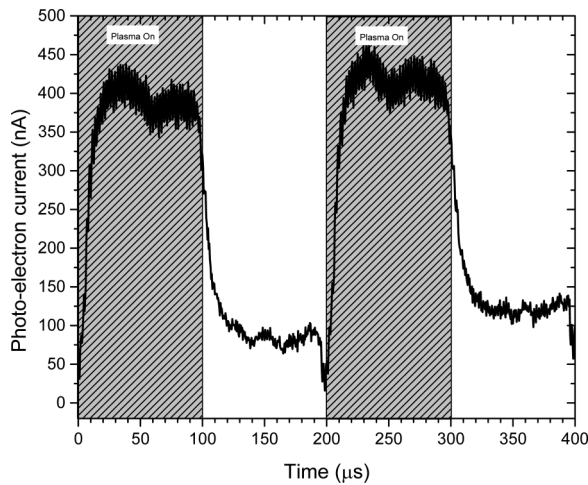


FIG. 4. Time-resolved photoelectron current through the gold film for a pulsed Ar/He VUV source ICP. Pulsing frequency = 5 kHz, duty cycle = 50%, period-averaged power = 200 W. VUV source flow rates were 2.5 SCCM Ar and 47.5 SCCM He. 250 SCCM Ar was injected into the downstream chamber (no plasma) where it mixed with the output gas from the VUV source. Downstream pressure = 60 mTorr. Substrate bias = -13 V_{DC}. Twenty-point smoothing (adjacent averaging) was used to reduce noise induced by the plasma.

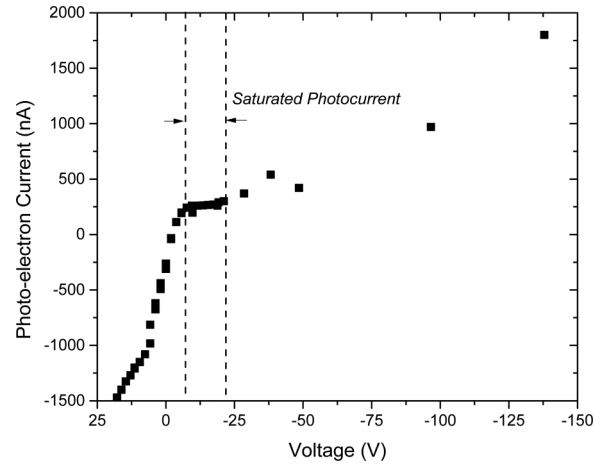


FIG. 5. Photoelectron current through the Au thin film for a continuous wave 200 W VUV source plasma with 47.5 SCCM He and 2.5 SCCM Ar. An additional 250 SCCM Ar was added to the etching chamber (no plasma) and the downstream pressure was 60 mTorr. The estimated pressure in the VUV source was 277 mTorr.

of the accelerated photoelectrons leaving the surface with the Ar gas inside the cage, resulting in an increasing positive ion current.

The measured photoelectron current, I_{pe} , produced when multiple wavelengths of light are incident on the Au surface is given by the relationship

$$I_{pe} = t_{grid} A e \sum_{i=1}^n Y_i^{Au} f_i, \quad (2)$$

where Y_i^{Au} is the Au photoemission yield for emission line i , f_i is the absolute photon flux for line i , t_{grid} ($=0.81$) is the transmission of the grid above the Au detector, A ($=3.14 \text{ cm}^2$) is the area of the Au detector, and e is the elemental charge. f_i is simply the total photon flux, f_{ph} , multiplied by the fraction, δ_i , of the total light for each line i , determined from spectra such as those in Figs. 2(a) and 2(b), with a known relative intensity calibration (in this case a constant sensitivity over the small range of wavelengths, as stated above). Therefore, the total absolute photon flux is given by

$$f_{ph} = \frac{I_{pe}}{t_{grid} A e \sum_{i=1}^n Y_i^{Au} \delta_i}. \quad (3)$$

Using the average intensities in the spectra in Figs. 2(a) and 2(b) for emissions from Ar I at 104.82 and 106.67 nm, Ar II at 92.0 and 93.2 nm, and N at 113.5 nm, and ignoring other weaker lines, $\sum_{i=1}^n Y_i^{Au} \delta_i = 0.064$. Finally, using the average of the values for the published photoemission yields (defined as the number of electrons ejected from the surface divided by the number of incident photons, see above), $\sum_{i=1}^n Y_i^{Au} \delta_i = 0.048$.

Figures 6–8 present the saturated photoemission currents with a -13 V bias applied to the substrate and absolute photon fluxes computed from Eq. (2), as a function of power, percent Ar, and downstream pressure, respectively.

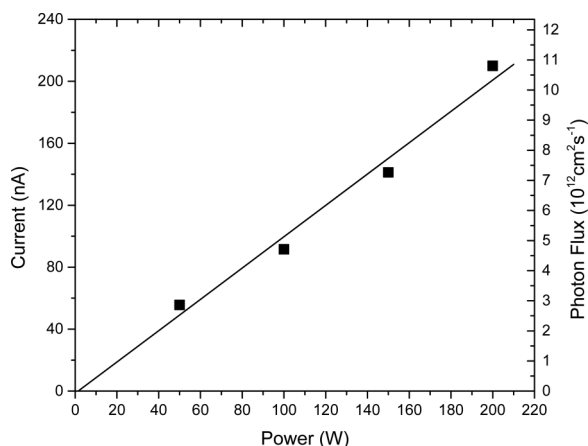


FIG. 6. Saturated photoelectron current with -13 V bias on the Au substrate as a function of VUV source power, with 47.5 SCCM He and 2.5 SCCM Ar. An additional 250 SCCM Ar was added to the etching chamber (no plasma) and the downstream pressure was 60 mTorr. The estimated pressure in the VUV source was 277 mTorr. The solid line is a least squares fit. The right axis is the calculated photon flux based on the photoelectron yield for the corresponding current.

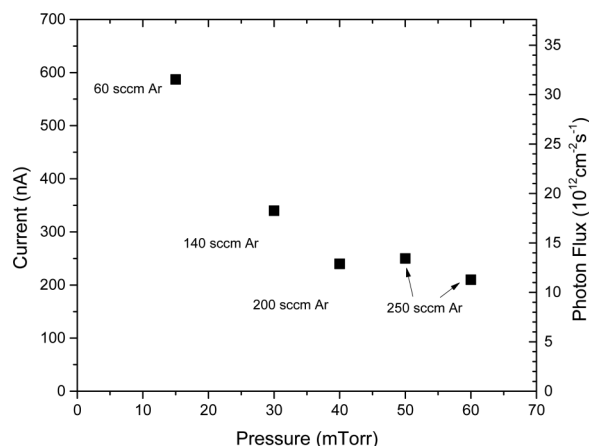


FIG. 8. Saturated photoelectron current with -13 V bias on the Au substrate as a function of measured downstream pressure. The VUV source feed gas was 47.5 SCCM He and 2.5 SCCM Ar at a power of 200 W. Between 60 and 250 SCCM, Ar was added to the downstream chamber (no plasma), as indicated by the labels in the figure. The estimated VUV source pressure was a nearly-constant 270–277 mTorr between 15 and 60 mTorr downstream pressures. Downstream pressure was adjusted by throttling the gate valve.

C. Discussion

The photon flux in Fig. 6 increases linearly with power, as would be expected. This is consistent with the spectrometer measurements at 5%Ar given in Fig. 3. Titus *et al.* also found a near linear dependence of total VUV light intensity in 10 and 20 mTorr pure Ar ICPs.³⁸ For the measurements in Fig. 6, the Ar partial pressure was 13.8 mTorr, hence the linear trend with power reported

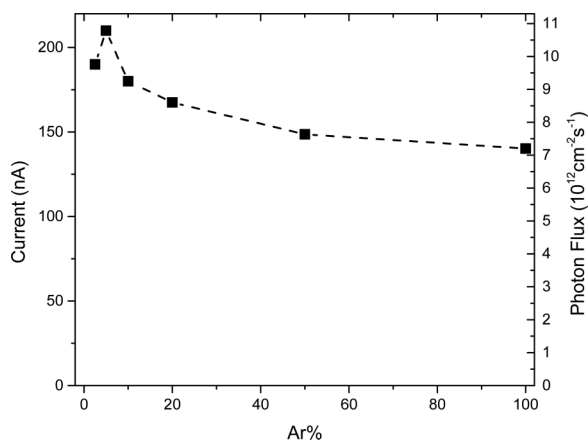


FIG. 7. Saturated photoelectron current with -13 V bias on the Au substrate as a function of %Ar, with a constant 50 SCCM He plus Ar flow rate, and 200 W power. An additional 250 SCCM Ar was added to the etching chamber (no plasma) and the downstream pressure was 60 mTorr. The estimated pressure in the VUV source was 277 mTorr.

here is in agreement with the results of Titus *et al.* Boffard *et al.* also found a linear increase with power in an Ar ICP at 15 mTorr up to about 150 W and then a sub-linear increase up to 1000 W.²⁵

In Fig. 7, the photon flux first increased as the Ar percentage increased, and then fell between 5% and 100% Ar. While this trend was also consistent with the sum of 104.82 and 106.67 nm emission at 200 W in Fig. 3, the magnitude of the rise and fall of emission intensity measured with the spectrometer was much greater than the photon flux measurements in Fig. 7. First, the trend measured with the spectrometer between Ar partial pressures of 6.9 and 27.7 mTorr (2.5%–10% Ar in Fig. 3) is similar to that reported by Boffard *et al.* for Ar ICPs between 5 and 25 mTorr pressure.²⁵ Radiation trapping, where photons are repeatedly absorbed and re-emitted until escaping at the edge of the chamber, is important in all these investigations.^{25,27} It is likely responsible for the severe falloff in $1s_4$ emission with increasing Ar partial pressure (Fig. 3), relative to that from $1s_2$. Tian and Kushner modeled the behavior of VUV radiation from an Ar ICP and found similar trends with pressure.²⁷ They computed large trapping factors (the ratio of the effective lifetime including reabsorption to the natural lifetime of the excited state) for the 106.67 nm line while that of 104.82 nm emission line remained unchanged. Consequently, this explains why the photon flux measurements in Fig. 7 are a much better match to the $1s_2$ emission intensities in Fig. 3 than to the combined $1s_2 + 1s_4$ emission intensity: the added Ar downstream traps most of the 106.67 nm light emitted by the upstream ICP (VUV source).

Radiation trapping also explains why the photon flux decreases as a function of increasing downstream Ar pressure at near-constant upstream pressure in the VUV source, as shown in Fig. 8.

Though the main motivation for this study was to determine the absolute flux of additional VUV photons from the VUV source that are incident on a Si sample during etching in the downstream ICP, it is also of interest to compare the magnitude of light incident on the top of the honeycomb separator in the VUV source to reported intensities of light produced in other Ar ICPs. An attenuation factor can be defined as the ratio of light incident on the plane at the top of the honeycomb-to-the light incident on the plane at the grid just above the Au sample. If we assume a cosine distribution of light incident on the honeycomb, and further assume that the tubes in the honeycomb cut-off light at angles greater than an angle equal to the arctan of the ratio of tube radius to length (2 mm/30 mm), account for the 40% open area of the honeycomb and grid combination, and further account for the roughly 2 times larger diameter of the light spot reaching the sample (i.e., 4 times the area), then the total attenuation factor is $1/(0.067 \times 0.4 \times 0.25) \sim 150$.

The highest intensity (3.2×10^{13} photons/cm² s) in the present study was for a 200 W power and 15 mTorr downstream pressure with a 5% Ar/He mixture at an estimated VUV source pressure of 274 mTorr, corresponding to an Ar partial pressure of about 13.7 mTorr (Fig. 8, upper left point). This would then correspond to a photon flux at the edge of the ICP of $150 \times 3.2 \times 10^{13} = 5 \times 10^{15}$ photons/cm² s. Woodworth *et al.* measured the VUV spectra of an Ar ICP.²⁴ The highest VUV photon flux at 200 W and 20 mTorr was $\sim 3.1 \times 10^{16}$ photons/cm² s through a hole in the center of a Si wafer and about 2×10^{15} photons/cm² s when observed through a side port. Titus *et al.* measured a flux of 1×10^{16} photons/cm² s in a 10 mTorr, 200 W Ar ICP.³⁸ Jinnai *et al.* combined an on-wafer monitor with a neural network model to predict the plasma VUV emission.¹⁰ For pure Ar ICP (typical operating conditions of 1000 W and 5 mTorr), the highest VUV emission flux was estimated to be about 1.5×10^{15} photons/cm² s near the substrate. Boffard *et al.* measured the VUV flux and the Ar 1s₂ and 1s₄ resonant state densities in an Ar ICP.²⁵ The highest photon flux was found to be 9×10^{16} cm² s⁻¹ at 600 W and 10 mTorr. Iglesias *et al.* used a sodium salicylate (NaSal) detector to measure the VUV emission of microwave Ar/O₂ plasmas.²⁶ The re-emitted fluorescence of NaSal in the UV/VIS spectral range was used to deduce a VUV radiation intensity (<112 nm) of about 1.6×10^{15} /cm² s in a pure Ar plasma at 1500 W and 190 mTorr. Tian and Kushner reported a computational study of VUV emission in Ar/Cl₂ ICP. In pure Ar, they predicted a flux of about 1.1×10^{16} photons/cm² s.²⁷ In summary, given the differences in geometries, power densities, and experimental uncertainties, the photon fluxes measured in the present study are, therefore, within reasonable agreement with the range of values reported for Ar ICPs.

IV. SUMMARY AND CONCLUSIONS

A new method was presented for measurement of the absolute flux of VUV photons produced by an inductively coupled plasma (VUV source). Optical emission spectra from this reactor (fed by an Ar/He mixture), attached to a differentially pumped VUV monochromator, showed relatively strong emissions at 104.82 and 106.67 nm, corresponding to the 1s₂ and 1s₄ resonant states of Ar, respectively. Light from the VUV source was allowed to strike a gold film, and the resulting electron photoemission current was measured.

The absolute VUV photon flux was then deduced from the known photoemission yield of gold. VUV source plasma power and gas composition were varied to find the maximum Ar VUV emission intensity at 104.82 and 106.67 nm. A comparison between the integrated intensity of the Ar VUV emission with the photocurrent through the gold film suggested that the photocurrent was mostly from the Ar 1s₂ and 1s₄ resonant states. The highest VUV photon flux to the substrate surface was found to be 3.2×10^{13} photons/cm² s when the VUV source power was 200 W, the feed gas was 2.5 SCCM Ar and 47.5 SCCM He, and that to the etching chamber was 60 SCCM Ar, and downstream ICP pressure of 15 mTorr. When adjusted for differences in operating and geometric conditions, the photon flux measured in this work was comparable to that reported in the literature. The absolute VUV photon flux measurement by monitoring the photocurrent through a gold thin film was demonstrated to be a feasible and simple method. Using the measured photon fluxes in this study, the absolute yield of p-type Si atoms etched per VUV photon in a chlorine-containing plasma was obtained and will be reported in a separate publication.¹⁹

ACKNOWLEDGMENTS

This work was supported financially by the National Science Foundation (No. PHY-1500518) and the Department of Energy (DOE), Office of Fusion Energy Science (No. DE-SC0001939).

Conflict of Interest

The authors have no conflicts of interest to disclose.

DATA AVAILABILITY

The data that support the findings of this study are available within the article.

REFERENCES

- 1V. M. Donnelly and A. Kornblit, *J. Vac. Sci. Technol. A* **31**, 050825 (2013).
- 2F. A. Houle, *Phys. Rev. B* **39**, 10120 (1989).
- 3W. Sesselmann, E. Hudeczek, and F. Bachmann, *J. Vac. Sci. Technol. B* **7**, 1284 (1989).
- 4T. N. Rhodin and C. Paulsen-Boaz, *Prog. Surf. Sci.* **54**, 287 (1997).
- 5N. Van Hieu and D. Lichtman, *J. Vac. Sci. Technol. A* **1**, 1 (1983).
- 6E. Ekwelundu and A. Ignatiev, *Surf. Sci.* **179**, 119 (1987).
- 7T. Yunogami, T. Mizutani, K. Suzuki, and S. Nishimatsu, *Jpn. J. Appl. Phys.* **28**, 2172 (1989).
- 8T. Tatsumi, S. Fukuda, and S. Kadomura, *Jpn. J. Appl. Phys.* **33**, 2175 (1994).
- 9S. Samukawa, Y. Ishikawa, S. Kumagai, and M. Okigawa, *Jpn. J. Appl. Phys.* **40**, L1346 (2001).
- 10B. Jinnai, S. Fukuda, H. Ohtake, and S. Samukawa, *J. Appl. Phys.* **107**, 043302 (2010).
- 11D. Nest, D. B. Graves, S. Engelmann, R. L. Bruce, F. Weillboeck, G. S. Oehrlein, C. Andes, and E. A. Hudson, *Appl. Phys. Lett.* **92**, 153113 (2008).
- 12B. Jinnai, T. Nozawa, and S. Samukawa, *J. Vac. Sci. Technol. B* **26**, 1926 (2008).
- 13S. Uchida, S. Takashima, M. Hori, M. Fukasawa, K. Ohshima, K. Nagahata, and T. Tatsumi, *J. Appl. Phys.* **103**, 073303 (2008).
- 14S. Tian, V. M. Donnelly, and D. J. Economou, *J. Vac. Sci. Technol. B* **33**, 030602 (2015).
- 15A. Kazor and I. W. Boyd, *Appl. Surf. Sci.* **54**, 460 (1992).
- 16I. W. Boyd, V. Craciun, and A. Kazor, *Jpn. J. Appl. Phys.* **32**, 6141 (1993).

- ¹⁷G. Y. Park, S. J. Park, M. Y. Choi, I. G. Koo, J. H. Byun, J. W. Hong, J. Y. Sim, G. J. Collins, and J. K. Lee, *Plasma Sources Sci. Technol.* **21**, 043001 (2012).
- ¹⁸W. Zhu, S. Sridhar, L. Liu, E. Hernandez, V. M. Donnelly, and D. J. Economou, *J. Appl. Phys.* **115**, 203303 (2014).
- ¹⁹L. Du, D. J. Economou, and V. M. Donnelly, *J. Vac. Sci. Technol. B* **40**, 022207 (2022).
- ²⁰H. Shin, W. Zhu, V. M. Donnelly, and D. J. Economou, *J. Vac. Sci. Technol. A* **30**, 021306 (2012).
- ²¹S. Sridhar, L. Liu, E. W. Hirsch, V. M. Donnelly, and D. J. Economou, *J. Vac. Sci. Technol. A* **34**, 061303 (2016).
- ²²E. W. Hirsch, L. Du, D. J. Economou, and V. M. Donnelly, *J. Vac. Sci. Technol. A* **38**, 023009 (2020).
- ²³L. Du, E. W. Hirsch, D. J. Economou, and V. M. Donnelly, *J. Vac. Sci. Technol. A* **38**, 053003 (2020).
- ²⁴J. R. Woodworth, M. E. Riley, V. A. Amatucci, T. W. Hamilton, and B. P. Aragon, *J. Vac. Sci. Technol. A* **19**, 45 (2001).
- ²⁵J. B. Boffard, C. C. Lin, C. Culver, S. Wang, A. E. Wendt, S. Radovanov, and H. Persing, *J. Vac. Sci. Technol. A* **32**, 021304 (2014).
- ²⁶E. J. Iglesias, F. Mitschker, M. Fiebrandt, N. Bibinov, and P. Awakowicz, *Meas. Sci. Technol.* **28**, 085501 (2017).
- ²⁷P. Tian and M. J. Kushner, *Plasma Sources Sci. Technol.* **24**, 034017 (2015).
- ²⁸S. Espinho, E. Felizardo, J. Henriques, and E. Tatarova, *J. Appl. Phys.* **121**, 153303 (2017).
- ²⁹L. R. Peterson and J. E. Allen, *J. Chem. Phys.* **56**, 6068 (1972).
- ³⁰J. Welty, C. E. Wicks, G. L. Rorrer, and R. E. Wilson, *Fundamentals of Momentum, Heat, and Mass Transfer*, 5th ed. (Wiley, New York, 2007).
- ³¹J. A. R. Samson, *Techniques of Vacuum Ultraviolet Spectroscopy* (Pied Publ., Nebraska, 1967, 1980), pp. 212–216.
- ³²R. B. Cairns and J. A. R. Samson, *J. Opt. Soc. Am.* **56**, 1568 (1966).
- ³³W. F. Krolikowski and W. E. Spicer, *Phys. Rev. B* **1**, 478 (1970).
- ³⁴B. Feuerbacher and B. Fitton, *J. Appl. Phys.* **43**, 1563 (1972).
- ³⁵B. R. Cooper, H. Ehrenreich, and H. R. Philipp, *Phys. Rev.* **138**, A494 (1965).
- ³⁶H. Shin, W. Zhu, D. J. Economou, and V. M. Donnelly, *J. Vac. Sci. Technol. A* **30**, 031304 (2012).
- ³⁷V. M. Donnelly, *J. Phys. D Appl. Phys.* **37**, R217 (2004).
- ³⁸M. J. Titus, D. Nest, and D. B. Graves, *Appl. Phys. Lett.* **94**, 171501 (2009).